THE ASTROPHYSICAL JOURNAL, 555:1013–1019, 2001 July 10

EXCITATION OF THE GANYMEDE ULTRAVIOLET AURORA

AHARON EVIATAR[1,2]
Laboratory for Extraterrestrial Physics, Code 692, NASA Goddard Space Flight Center, Greenbelt MD 20771; arkee@daphne.tau.ac.il
DARRELL F. STROBEL
Department of Earth and Planetary Sciences and Department of Physics and Astronomy, Johns Hopkins University, Baltimore, MD 21218
BRIAN C. WOLVEN AND PAUL D. FELDMAN
Department of Physics and Astronomy, Johns Hopkins University, Baltimore, MD 21218
MELISSA A. MCGRATH
Space Telescope Science Institute, 3700 San Martin Drive, Baltimore, MD 21218
AND
DONALD J. WILLIAMS
Johns Hopkins University Applied Physics Laboratory, Laurel, MD 20742
Received 2000 December 4; accepted 2001 March 19

ABSTRACT

We analyze the ultraviolet aurorae observed on Ganymede by means of the *Hubble Space Telescope* and compare them to similar phenomena on Earth. We find that the tenuous nature of Ganymede's atmosphere precludes excitation of the aurora by high-energy electrons and requires a local acceleration mechanism. We propose the following as plausible mechanisms for generating both the continuous background emission and the intense auroral bright spots:

1. Birkeland-type currents and associated magnetic field–aligned electric fields.
2. The stochastic heating of plasma electrons by the Landau damping of electron plasma oscillations generated by precipitated energetic electrons.

We conclude that the electron density in the bright regions may attain local values as high as 10^5 cm^{-3}.

Subject headings: planets and satellites: individual (Ganymede) — plasmas — ultraviolet: solar system

1. INTRODUCTION

In recent years, observations of Ganymede in the ultraviolet by means of the *Hubble Space Telescope* (*HST*) together with particles and fields measurements carried out in situ by experiments on the *Galileo* orbiter have led to a new understanding of the nature of Ganymede's atmosphere and its relation to both the underlying surface and the surrounding magnetosphere. The ultraviolet aurora was discovered by Hall et al. (1998) and observed in greater detail by Feldman et al. (2000). Energetic electron data from the magnetosphere of Ganymede were obtained from the energetic particle detector (EPD) on board *Galileo* (Williams, Mauk, & McEntire 1997a; Williams et al. 1997b; Williams & Mauk 1997; Paranicas et al. 1999; Eviatar et al. 2000). The topology of the intrinsic magnetic field of Ganymede has been studied in detail by the *Galileo* magnetometer team (Kivelson et al. 1998 and references therein). In this paper we shall attempt to combine those data sets that are relevant to the creation of the aurora and to investigate the relationship between the spatial structure of the aurora and that of the magnetospheric configuration that controls it. We shall propose various scenarios for the excitation of the observed emissions and discuss the implications thereof.

2. ULTRAVIOLET AURORA

Observations of emission in the ultraviolet lines of atomic oxygen were reported by Hall et al. (1998) and by Feldman et al. (2000) at wavelengths of 1304 and 1356 Å. Monochromatic images of Ganymede in O I λ1356, obtained with the Space Telescope Imaging Spectrograph (STIS) on board *HST*, were presented by Feldman et al. (2000) and are reproduced in Figure 1, which is taken from the above paper. A summary of the observations and exposure parameters may be found in Feldman et al. (2000). Ganymede's sub-Earth longitude (the geocentric orbital phase) varied from 290° to 300° during the course of the STIS observations; the "upstream" direction relative to the incident Jovian corotational plasma flow is along the 270° meridian, which is slightly to the right of Ganymede's center in the images of Figure 1.

3. PRODUCTION OF THE AURORA

In this section we shall explore the physical mechanisms that we consider to be possible sources of the observed aurora. The *HST* images show bright spots at about 45° latitude with a drop-off in intensity toward the pole (Feldman et al. 2000) of about the same factor of 5 as seen in the energetic electron intensity, as may be noted below in Figure 4. The aurorae observed by Feldman et al. (2000) consist of a background emission above the detection limit of 50 R (1 R = 10^6 photons cm^{-2} s^{-1}) but not exceeding 100 R over most of the auroral oval region. Superposed on this background are localized regions of emission of intensity up to and even exceeding 300 R (see Fig. 1).

3.1. *Model Constraints*

As discussed in the observation papers (Hall et al. 1998; Feldman et al. 2000), the intensity ratio of the detected O I λ1356 and λ1304 provides convincing evidence for O_2 as the

[1] National Academy of Science/National Research Council Senior Research Associate.
[2] On sabbatical leave from the Department of Geophysics and Planetary Sciences, The Raymond and Beverly Sackler Faculty of Exact Sciences, Tel Aviv University, Ramat Aviv, Israel.

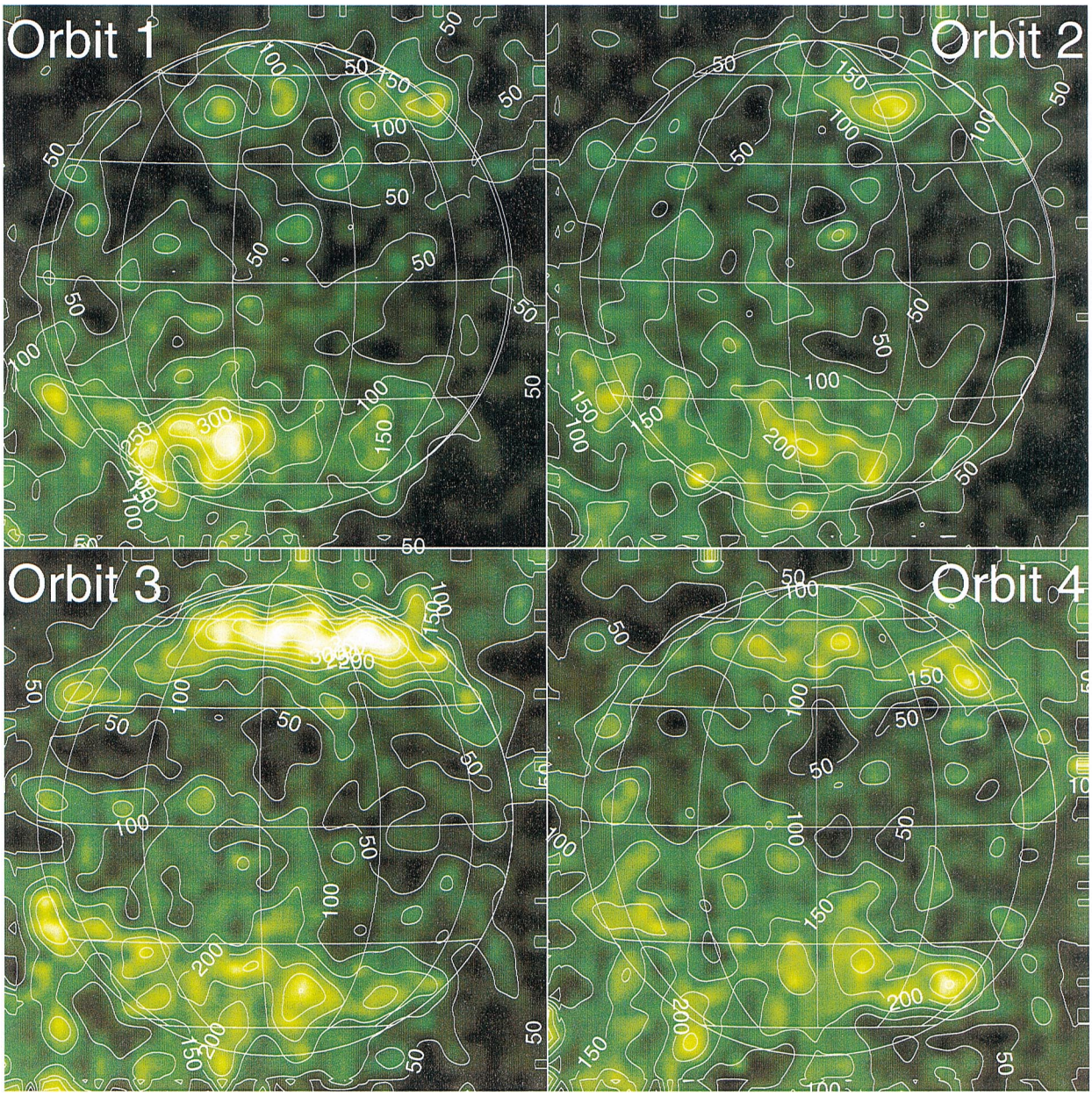

FIG. 1.—Images of Ganymede's O I λ1356 emission for each of the four *HST* orbits on 1998 October 30. The "upstream" direction relative to the incoming plasma flow is along the 270° meridian, which is slightly to the right of disk center in each of the images above. The emission below and to the left of Ganymede is solar C II radiation reflected from Ganymede's disk. This figure appeared in a previous publication (Feldman et al. 2000).

dominant constituent of Ganymede's atmosphere. This is consistent with the prediction of the ionosphere model of Eviatar, Vasyliūnas, & Gurnett (2001). The brightest emission of O I λ1356 reaches peak intensities of $\sim$300 R in the auroral oval/separatrix regions on Ganymede. Emission cross sections for O I λ1356 by the electron impact on O_2 are unfortunately poorly measured because of the long radiative lifetime of the O I ($3s\ ^5S^0$) term, $\approx$200 μs. Cascade from the O I ($3p\ ^5D$) term with the emission of a 7774 Å photon provides a lower limit to the total emission cross section and is assumed to characterize the cross section shape above 100 eV (Erdman & Zipf 1987). We used Wells, Borst, & Zipf (1971) to define the cross section shape from 20 to 100 eV and normalized the emission cross section at 100 eV to 7×10^{-18} cm^2, as given in Itikawa et al. (1989). As an independent check, we also used some recent preliminary unpublished emission cross section measurements for O I λ1356 and O I λ1304 (J. Ajello 2000, private communication) and found no significant differences in the emission rates given below.

To define the densities and temperatures of the electron population required to explain the peak emission intensities observed in Ganymede's auroral region, we used a model atmosphere similar to that constructed by Feldman et al. (2000) with a surface O_2 density of 1×10^8 cm^{-3} and a vertical column density of 2.5×10^{14} cm^{-2}, which is the abundance upper limit deduced from the UV stellar occultation observed by *Voyager* (Broadfoot et al. 1981). The model neutral atmosphere computed by Eviatar et al. (2001) predicts a significantly lower O_2 column density, and the conclusions reached here hold a fortiori for that atmosphere.

In what follows, the radial distance from the center of Ganymede r is expressed in Ganymede radii ($1R_G = 2634$ km), and temperature is expressed in energy units. We divide the atmosphere into two regions, one close ($r \le r_c = 1.38R_G$ or 3634 km) to the surface, to which a Bates (1959) atmosphere model is applied, and an exosphere region in which a coronal model is used:

$$n_{O_2}(r) = \begin{cases} n_{O_2}(1)\left[\dfrac{1-\eta}{\exp(\tau\Phi)-\eta}\right]^{1+\Gamma} \exp(\tau\Phi), & r \le r_c, \\ n_{O_2}(r_c)\left(\dfrac{1+r_c}{1+r}\right)^2 \exp\left[-\dfrac{r-r_c}{H(r_c)}\right], & r > r_c. \end{cases} \quad (1)$$

In equation (1), $T_0 = 0.011$ eV is the surface temperature, $T_{inf} = 0.086$ eV is the exosphere temperature,

$$\eta = \frac{T_{inf} - T_0}{T_{inf}}$$

is the temperature gradient scale,

$$\tau = \frac{1}{\eta T_{inf}} \frac{dT}{dr}$$

is taken to be 10^{-4} cm^{-1}, the gravipotential radial distance is given by

$$\Phi = R_G\left(\frac{r-1}{r}\right),$$

the scale height is $H_2(r) = [T(r)/mg(r)]$, and the ratio of the temperature gradient to the scale height is given by $\Gamma = [1/\tau H_2(1)]$, which is equal to 0.4851 for this set of parameters.

Plasma wave instrument (PWS) measurements along the G1 and G2 *Galileo* spacecraft trajectories (Gurnett et al. 1996; Eviatar et al. 2001) were used to construct an electron density profile. The G2 measurements were made much closer to the surface than the G1 measurements and showed a sharp change in slope near the closest approach at 261 km (Eviatar et al. 2001). The fit was made to the PWS measurements with a scale height of 125 km near Ganymede and a scale height of 600 km farther out. This fit extrapolates to a surface electron density of 2500 cm^{-3}. If we were to extrapolate the density to the magnetic field magnitude, which is conserved for constant flow along a field line, as shown in Figure 4 of Eviatar et al. (2001), the surface density would be about 300 cm^{-3}. We should note, however, that the figure in the above paper shows a major violation of n/B conservation near the closest approach, which may indicate that the conditions for conservation, notably, constant speed along the field line, do not hold in the lower atmosphere. These model O_2 and electron density profiles are illustrated in Figure 2.

In Figure 3 the O I λ1356 emission brightness is calculated as a function of electron temperature with the model atmosphere and ionosphere in Figure 2 and the O I λ1356 total emission cross section discussed above, under the assumption of prompt emission. This is an excellent assumption in such a thin atmosphere, in which the collision time constant at the assumed surface density is on order of 10 s [O-O_2 collision cross section times velocity $\le 10^{-9}$ cm^3 s^{-1}, $n(O_2) \approx 10^8$ cm^{-3}]. For the low-density case, only if the entire electron population is characterized by a Maxwellian distribution with temperature in the range of 75–300 eV can the observed 300 R intensity be attained. Even at the peak emission rate at 150–200 eV, almost all electrons would have to be suprathermal. Thus, unless the *Voyager* epoch upper limit on the O_2 atmosphere is not applicable during the *Galileo* epoch or there are considerably more electrons than inferred from the *Galileo* measurements (Gurnett et al. 1996; Eviatar et al. 2001), the bulk of those ambient electrons must be accelerated in the auroral oval/separatrix regions to account for the *HST* observed intensities at the bright spots. For the higher density cases, shown in Figure 3, creation of suprathermal tails or "bumps in tail" on the order of at least 10% of the main electron population would be required. In either case, a local acceleration is required. Possible mechanisms for this local acceleration will be discussed below. Similarly, it would be difficult to generate continuously the diffuse, broadly distributed limb emission of intensity between 50 and 100 R by precipitation of the 20 eV plasma sheet population even if the number density were consistently as high as the 20 cm^{-3} value seen by *Voyager* 2 at $13R_J$ (Scudder,

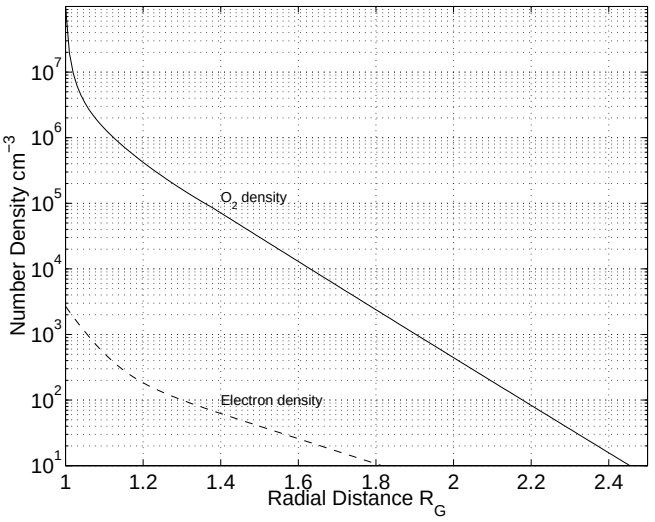

FIG. 2.—Calculated variation of O_2 and electron number density. The neutral molecular oxygen density is that calculated in eq. (1), and the electron density is fitted to the G2 encounter (Eviatar et al. 2001).

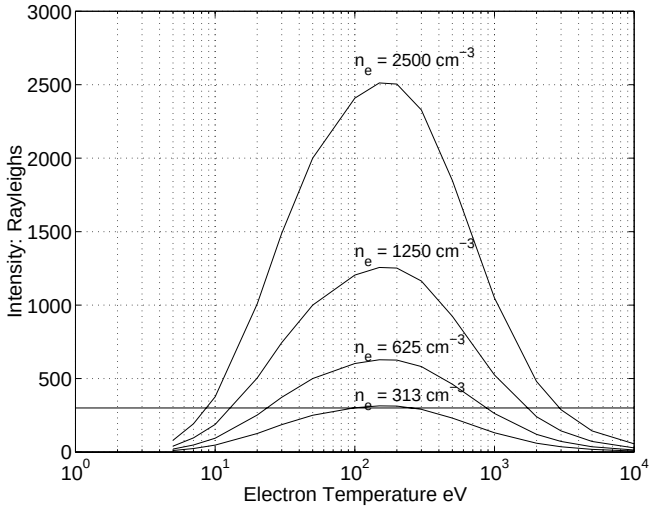

FIG. 3.—Calculated intensity of O I λ1356 emission. The 300 R value is marked to show the conditions required.

Sittler, & Bridge 1981), although a contribution to the emission by this component cannot be ruled out totally.

3.2. *Terrestrial Analog*

It is of interest to compare the Ganymede and terrestrial UV aurorae. They have in common a latitudinal distribution characterized by an "oval" of enhanced intensity. These are the regions that receive the maximal intensity of particle precipitation. Since in both cases the required power must be imparted to the particles by local acceleration, it is useful to consider the terrestrial case as an analog.

Kauristie et al. (1999) compare electron precipitation measurements from the *Viking* spacecraft with Defense Meteorological Satellite Program UV observations. They find that the correspondence between the boundaries of the UV and the electron precipitation is significant but by no means perfect and that differences can occur. Obviously, we do not have enough information on Ganymede to make these comparisons with the same degree of detail. Another feature that seems to be shared is the decrease of the energetic electron flux with increasing latitude poleward of the oval so that the precipitation becomes a weak "polar rain" over the pole (see Fig. 4). Both objects show a massive escape of ionospheric plasma along auroral field lines. It is known that this escape is associated with heating and acceleration of auroral electrons (Lundin 1988). The outflow observed by Frank et al. (1997) begins to increase as the spacecraft moves toward higher latitude and enters the polar cap region. The composition and speed given therein are not correct (Vasyliūnas & Eviatar 2000; Eviatar et al. 2001); i.e., Frank et al. (1997) interpret their fluxes as protons flowing at 70 km s^{-1}, whereas Eviatar et al. (2001) show that there is practically no atomic hydrogen in the polar atmosphere and that the ionization time is long compared to the escape time. The outflow is O^+ at 18 km s^{-1}, which is consistent with the present observations. Nonetheless, the *Galileo* fluxes and times are consistent with the spacecraft's being in the auroral region. The reconnection on the upstream side increases the amount of open flux and expands the polar cap with energy being stored in the lobes. Release of this energy is associated with the acceleration and precipitation of electrons and the subsequent radiation. We must, however, bear in mind that a major difference between the atmospheres of Earth and Ganymede is the column density, which on Earth is many orders of magnitude greater than at Ganymede. It follows, thus, that the energetic electrons seen by the EPD experiment on *Galileo* (Paranicas et al. 1999; see Fig. 4) penetrate the atmosphere almost totally without collisions and impact the surface directly.

3.3. *Continuous Aurora*

The background emission is distributed around Ganymede; its maximum emission is about 100 R and is usually considerably less. Limb observations (Feldman et al. 2000) show intensities of no more than 100 R. It would appear on first impression reasonable to expect that this emission might reflect the general precipitation pattern of electrons impinging on Ganymede and its atmosphere in the open field line region. Eviatar et al. (2001) have developed a model of the polar Ganymedean ionosphere from which they estimate with nominal emission efficiency, obtained from Hall et al. (1998), that a steady state air glow or continuous aurora on the order of 20 R can be maintained without a further input of energy. In this region of the Jovian magnetosphere, the electron population in the plasma sheet was found by *Voyager* to be made up of a core population of enhanced density ($n_e \approx 5$–20 cm^{-3}) with a temperature of about 20 eV, a suprathermal halo of about 1/10 the number density, and a temperature of 2 keV (Scudder et al. 1981). This population can support at most an emission rate of about 10–40 R (or 3–12 R at 60° latitude). We must therefore rule out the possibility that local thermal electrons are creating the background emission. If proper conditions hold, the plasma sheet electrons observed by *Voyager* (Scudder et al. 1981) may contribute a significant fraction of the diffuse aurora. In general, however, it appears more plausible to attribute it to a local acceleration mechanism. In the following subsection, we shall analyze the generation of the discrete auroral hot spots, the mechanism for which will also suffice for the continuous background.

3.4. *Discrete Intense Aurora*

The hot spots of intense auroral emission cannot be generated by the plasma sheet electrons nor by the local electrons unless some effective acceleration operates to create the flux of lower energy electrons carrying a sufficient power flux to the atmosphere. The constraint of low energy derives from the tenuous nature of the atmosphere, which is incapable of stopping higher energy electrons whose cross sections for collisions with the ambient atmospheric particles are too low. The observation of higher intensity in the forbidden 1356 Å line (Hall et al. 1998; Feldman et al. 2000) precludes the possibility of excitation by electron impact in the ice regolith, which is in analogy to the proposed dissociation of O_2 by UV radiation in the ice matrix followed by creation of ozone (Calvin, Johnson, & Spencer 1996). Although the available information on low-energy electrons does not extend to energy below 800 eV (Paranicas et al. 1999), the densities of cold electrons reported by Eviatar et al. (2001) indicate that there exists a source of electrons that could provide the needed auroral power if a local mechanism of acceleration could be found. In the following subsection we shall propose two plausible electron acceleration mechanisms.

3.5. *Stochastic Acceleration*

A possible means of excitation of the aurora, i.e., acceleration of the ambient particles, is stochastic acceleration by electrostatic waves. Plasma wave measurements made at Ganymede (Gurnett et al. 1996; Kurth et al. 1997) show a significant amplitude of such waves in the parts of the magnetosphere of Ganymede traversed by *Galileo* during its first two Ganymede encounters. The stochastic acceleration of charged particles by waves is discussed in detail in Melrose (1970), to which the reader is referred for details. In Figure 4 we show the depletion of EPD electrons during the Ganymede 2 encounter as the spacecraft moved in latitude. While, as shown above, these electrons cannot be the direct excitation agents of the observed auroral emissions, they can generate unstable electron plasma oscillations (Stix 1992) either by means of Cerenkov emission, the anisotropy created by the loss cone shown in Figure 5, or by the classic two-stream process. In any case, energy goes from the energetic particles to the waves, which in turn are Landau-damped by the thermal particles, some fraction of which

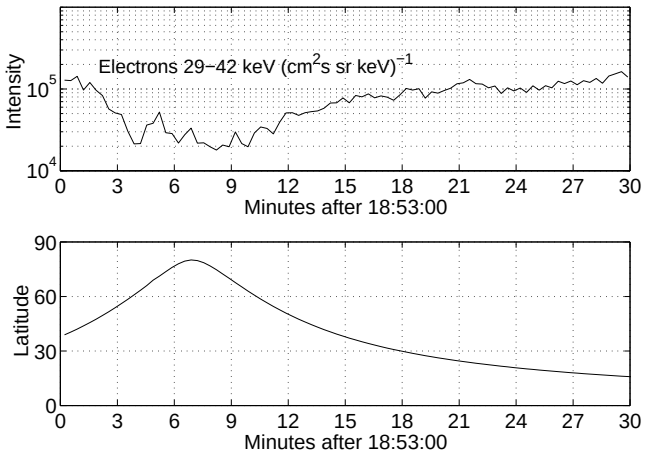

FIG. 4.—*Top*: Intensity of electrons observed in the given energy channel by the *Galileo* EPD instrument during the polar pass of G2. *Bottom*: Latitude of the spacecraft at the times corresponding to the observations shown in the top panel.

become suprathermal as required and go on to excite the emission via ionization and dissociative excitation of O_2.

It is shown by Melrose (1970) that nonrelativistic particles are accelerated by waves having a specific phase velocity

$$v \approx \frac{\omega_p}{k} ,$$

where k is the wavenumber and ω_p is the plasma frequency. The rate of gain of energy is approximately equal to the damping rate of the waves times the ratio of density of the energetic to thermal particles,

$$\frac{1}{w}\frac{dw}{dt} = \gamma_L(\boldsymbol{k}) .$$

Integration over the wave and particle energy spectra gives

$$\gamma_L(\boldsymbol{k}) = \int d^3\boldsymbol{p} w^l(\boldsymbol{p},\boldsymbol{k})\hbar\boldsymbol{k}\cdot\frac{\partial f(\boldsymbol{p})}{\partial \boldsymbol{p}}$$

$$\approx \frac{\pi}{2}\omega_p \frac{n_1(v)}{n} , \qquad (2)$$

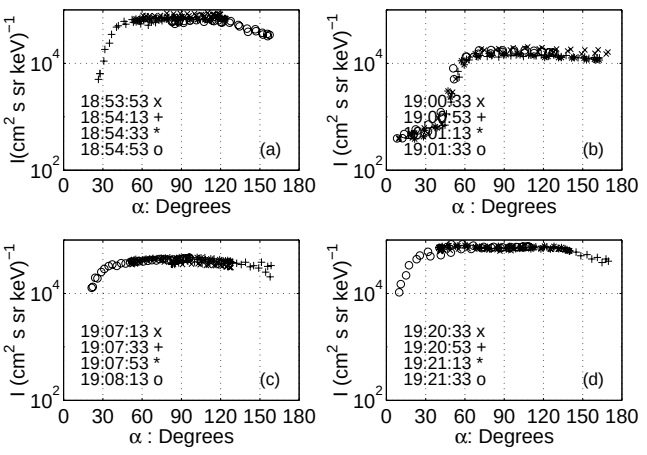

FIG. 5.—Local pitch angle distributions of EPD electrons along the G2 trajectory

where the integration is over momentum space, $w^l(\boldsymbol{p},\boldsymbol{k})$ is the electron plasma wave emission probability (Melrose 1970), and $n_1(v)/n$, is the suprathermal (energy >800 eV) fraction. This latter value may be estimated from the spectra of Paranicas et al. (1999) and the observations reported by Eviatar et al. (2001) to be on the order of 10^{-6}. The plasma frequency near Ganymede has been reported to be on the order of 200 kHz (Kurth et al. 1997), which leads to an energization time of about 1 s, comparable to the time required for a 30–50 eV electron to transit the atmosphere and be lost in the surface. As noted above, collisional losses of energy in the atmosphere will be small, and it thus appears plausible that stochastic acceleration may be a significant contributor to the energy budget of the ultraviolet aurora.

3.6. *Electric Fields and Birkeland Currents*

An alternative mechanism is embodied in magnetic field–aligned electric fields and their associated Birkeland currents such as are seen on Earth. For this purpose, we invoke the rotation of Jupiter as the energy source and estimate the potential associated with the electric field imposed by the Jovian magnetosphere flow past Ganymede. The role of this field in the transport of energetic electrons in the magnetosphere of Ganymede has been considered by Eviatar et al. (2000). In this analysis, the magnetic field lines are labeled by means of the dimensionless parameter L, which satisfies

$$L = \frac{r}{R_G}\csc^2\theta .$$

We use a spherical coordinate system in which the coordinates (r,θ,ϕ) are measured from the center of Ganymede, the north pole, assumed for this discussion to coincide with the north magnetic pole, and the meridian at the nadir with respect to the incident Jovian corotation flow, respectively. The electric potential function is taken to be that used by Schulz (1991) and by Volland (1984), who dealt with the terrestrial magnetotail field, namely, that imposed by a uniform external field on a dielectric cylinder. These investigators found that a quadratic is the most appropriate power of L. In terms of these variables, we may express the electric potential inside and outside the closed field line region as

$$\psi = \begin{cases} \sqrt{3}\epsilon E_J b\left(\dfrac{L}{L_*}\right)^2 \sin\phi = \sqrt{3}\epsilon E_J b\left(\dfrac{r}{L_*}\right)^2 \\ \qquad\qquad \times \csc^4\theta \sin\phi , & L \le L_* \\ \sqrt{3}\epsilon E_J b\left(\dfrac{L_*}{L}\right)^{1/2} \sin\phi = \sqrt{3}\epsilon E_J b\left(\dfrac{L_*}{r}\right)^{1/2} \\ \qquad\qquad \times \sin\theta \sin\phi , & L \ge L_* , \end{cases} \qquad (3)$$

in which E_J is the Jovian corotation electric field, taken to be 18 mV m^{-1} (Volwerk et al. 1999), $L_* \approx 1.8$ is the equatorial distance in Ganymede radii of the outermost closed field line, which corresponds to a surface footprint colatitude of 48°, $b = 2R_G$ is the magnetopause radius, and ϵ is the mapping coefficient, i.e., the ratio between the tail field and the Jovian corotation field (Kennel & Coroniti 1975), estimated by Kivelson et al. (1998) to be 0.5, which corresponds to rapid reconnection. The electric field components derived from equation (3) by means of the relation

$\boldsymbol{E} = -\nabla\psi$ are (in the following coordinate system):

$$E_r = \begin{cases} -\sqrt{3}\epsilon E_J b\left[\dfrac{2r}{(L_* R_G)^2}\right] \csc^4\theta \sin\phi\,, & L \le L_*\,, \\ \sqrt{3}\epsilon E_J b\left(\dfrac{L_* R_G}{2r^3}\right)^{1/2} \sin\theta \sin\phi\,, & L \ge L_*\,, \end{cases}$$

$$E_\theta = \begin{cases} \sqrt{3}\epsilon E_J b\left[\dfrac{r}{(L_* R_G)^2}\right] 4 \csc^4\theta \cot\theta \sin\phi\,, & L \le L_*\,, \\ \sqrt{3}\epsilon E_J b\left(\dfrac{L_* R_G}{r^3}\right)^{1/2} \sin\theta \sin\phi\,, & L \ge L_*\,, \end{cases}$$

$$E_\phi = \begin{cases} -\sqrt{3}\epsilon E_J b\left[\dfrac{r}{(L_* R_G)^2}\right] \dfrac{\csc^4\theta}{\sin\theta} \cos\phi\,, & L \le L_*\,, \\ -\sqrt{3}\epsilon E_J b\left(\dfrac{L_* R_G}{r^3}\right)^{1/2} \cos\phi\,, & L \le L_*\,. \end{cases} \quad (4)$$

It is clear from equation (4) and Figure 6 that there is a discontinuity in E_θ at $L = L_*$. The electric fields derived from the above potential are usually taken in the terrestrial context to be normal to the magnetic field. It has been pointed out by Straus & Schulz (1976) and Schulz (1991) that this condition must be violated in the region of the auroral oval. This corresponds to $L = L_*$, i.e., the ionospheric footprint of the magnetic shell that extends to the magnetopause and the current sheet. Schulz (1991) notes that at the Earth this corresponds to the region of the so-called Birkeland currents driven through the ionospheric resistance by such parallel electric fields. Indeed, the appropriate discontinuity in the meridional component of the electric field is observed on Earth.

It is not clear that the tenuous ionosphere of Ganymede will provide the resistivity needed to maintain the field, but the spotty nature of the aurora indicates that such may be possible locally. The pickup conductance (Goertz 1980) in the auroral bright spots is estimated to be as large as ~ 100 mho for the maximum scenario case,

$$n_e = 313 \text{ cm}^{-3}\,,$$
$$T_e = 100 \text{ eV}\,.$$

By comparison, the Alfvén conductance (Neubauer 1980) is only ~ 1 mho, and the Coulomb collision contribution to the Pedersen conductance is similarly negligible in the bright spots. We may expect, therefore, that the estimated field magnitudes, on the order of tens of mV m^{-1} could, with the expected low efficiency, create the suprathermal electrons needed to power the auroral emission.

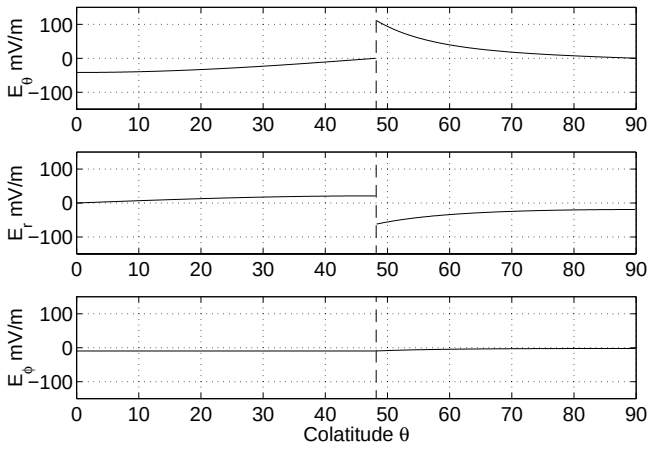

FIG. 6.—Components of the electric field in the northern hemisphere of Ganymede as a function of colatitude θ, evaluated at the surface. The radial and meridional components are the amplitudes of the azimuthal variation (see eq. [4]) evaluated in the plane parallel to the Jovian corotation flow, and the azimuthal component is evaluated in the plane normal to the flow.

To achieve the auroral bright spots of O I λ1356 emission with an intensity of 300 R consistent with the constraints on electron density and temperature illustrated in Figure 3, there must be a large associated ionization rate of the predominantly O_2 atmosphere. At the surface, the calculated ionization rate is $\sim 2 \times 10^{-5}$ s^{-1}, and the ion production rate is ~ 2000 cm^{-3} s^{-1}, whereas the column production rates of O_2^+ and O^+ by dissociative ionization are $\sim 4 \times 10^9$ and $\sim 6 \times 10^8$ cm^{-2} s^{-1}, respectively. Because the temperature characterizing the electron core distribution is unknown, we assume that the electrons recombine dissociatively with a typical rate applicable to the Earth's ionosphere, $\alpha_D \sim 2 \times 10^{-7}$ cm^3 s^{-1}. The surface electron density is, if production balances loss,

$$n_e = \left(\frac{2000}{\alpha_D}\right)^{1/2},$$

which is approximately 10^5 cm^{-3}. The implications of this very high density will be discussed below.

4. DISCUSSION

We have attempted to relate the UV O I aurora observed on Ganymede by Feldman et al. (2000) to possible interaction mechanisms with the magnetosphere of Jupiter. Since the ambient plasma sheet electrons (Scudder et al. 1981) do not suffice to generate even the relatively faint diffuse aurora, we conclude that a local acceleration mechanism, analogous to that operating on Earth, is needed to explain both the 300 R bright spots and the diffuse emission. We find that the tenuous nature of the upper atmosphere (Eviatar et al. 2001) makes direct impact excitation by the energetic electrons observed by *Galileo* (Williams et al. 1997a, 1997b; Paranicas et al. 1999) most ineffective. The high intensity of the λ1356 emission precludes excitation in the ice matrix itself, in which the high density would quench the forbidden line. The two possible mechanisms include stochastic acceleration by the collective plasma effects and the electric fields associated with magnetic field-aligned Birkeland currents. Strong electron plasma oscillations are observed by the *Galileo* PWS experiment (Gurnett et al. 1996; Kurth et al. 1997), and a simple quasi-linear calculation indicates that the rate of energization can be comparable to the rate of particle loss by impacting the surface, which renders this interaction plausible.

Since the bright spots are seen near the transition from open to closed field lines (Williams et al. 1997a; Eviatar et al. 2000; Kivelson et al. 1998), we consider the application of a terrestrial Birkeland current model first proposed by Straus & Schulz (1976). The meridional component of the electric field is found to show a discontinuity and a magnitude sufficient to provide the required electron fluxes. We suggest, therefore, that this mechanism is most likely to be the cause of the observed auroral high-intensity emissions on Ganymede, although the collective plasma acceleration process cannot be discounted as a contributing factor.

We have found that the extremely bright localized intensities imply a very high electron number density on the order of 10^5 cm^{-3}. Elevated electron temperatures in Gany-

mede's ionosphere would imply even larger densities. Transport processes such as ambipolar diffusion and polar wind acceleration in this thin atmosphere will decrease the electron density, but the inescapable conclusion is the prediction that in the hot spot auroral regions, the electron density must be significantly higher than elsewhere in the ionosphere. The value estimated here is much higher than the upper limit reported by Kliore (1998), but it should be kept in mind that these occultation observations were made at lower latitude. It should also be kept in mind that this prediction refers to local hot spot regions whose limited spatial dimensions would provide a radio path length that may be too short to create the column density needed to be detectable by *Galileo* radio occultation observations.

We gratefully acknowledge helpful discussions with David G. Sibeck and with Chris Paranicas. The work of A. E. at Goddard Space Flight Center/NASA was supported by the National Academy of Sciences/National Research Council under a Senior Research Associateship during the period 2000 May–December. His work on this problem began during a sojourn at the Space Telescope Science Institute under their Visiting Science Program during 2000 February–March. The hospitality of both institutions is gratefully acknowledged. The work of D. F. S. was supported by the National Space and Aeronautics Administration under grant NAG 5-4168. The work of B. C. W. and P. D. F. was supported in part by the National Space and Aeronautics Administration under grant NAS 5-30403 to Johns Hopkins University. The work at the Johns Hopkins University Applied Physics Laboratory was supported by the National Space and Aeronautics Administration by means of contract N00039-95-0002 between the US Department of the Navy and Johns Hopkins University.

REFERENCES

Bates, D. R. 1959, Proc. R. Soc. London A, 253, 451
Broadfoot, A. L., et al. 1981, J. Geophys. Res., 86, 8259
Calvin, W. M., Johnson, R. E., & Spencer, J. R. 1996, J. Geophys. Res. Lett., 23, 673
Erdman, P., & Zipf, E. C. 1987, J. Chem. Phys., 87, 4540
Eviatar, A., Vasyliūnas, V. M., & Gurnett, D. A. 2001, Planet. Space Sci., 49, 327
Eviatar, A., Williams, D. J., Paranicas, C., McEntire, R. W., Mauk, B. H., & Kivelson, M. G. 2000, J. Geophys. Res., 105, 5547
Feldman, P. D., McGrath, M. A., Strobel, D. F., Moos, H. W., Rutherford, K. D., & Wolven, B. C. 2000, ApJ, 535, 1085
Frank, L. A., Paterson, W. R., Ackerson, K. L., & Bolton, S. J. 1997, Geophys. Res. Lett., 24, 2151
Goertz, C. K. 1980, J. Geophys. Res., 85, 2949
Gurnett, D. A., Kurth, W. S., Roux, A., Bolton, S. J., & Kennel, C. F. 1996, Nature, 384, 535
Hall, D. T., Feldman, P. D., McGrath, M. A., & Strobel, D. F. 1998, ApJ, 499, 475
Itikawa, Y., et al. 1989, J. Chem. Phys. Ref. Data, 18, 23
Kauristie, K., Weygand, J., Pulkkinen, T. I., Murpree, J. S., & Newell, P. T. 1999, J. Geophys. Res., 104, 2321
Kennel, C. F., & Coroniti, F. V. 1975, Space Sci. Rev., 17, 857
Kivelson, M. G., et al. 1998, J. Geophys. Res., 103, 19, 963
Kliore, A. J. 1998, in Highlights of Astronomy, Vol. 11, ed. J. Anderson (Dordrecht: Kluwer), 1065
Kurth, W. S., Gurnett, D. A., Roux, A., & Bolton, S. J. 1997, Geophys. Res. Lett., 24, 2167
Lundin, R. 1988, Ann. Geophys., 6, 143
Melrose, D. B. 1970, Plasma Astrophysics (New York: Gordon & Breach)
Neubauer, F. M. 1980, J. Geophys. Res., 85, 1171
Paranicas, C., Paterson, W. R., Cheng, A. F., Mauk, B. H., McEntire, R. W., Frank, L. A., & Williams, D. J. 1999, J. Geophys. Res., 104, 17, 459
Schulz, M. 1991, in Geomagnetism, Vol. 4, ed. J. A. Jacobs (London: Academic), 87
Scudder, J. D., Sittler, E. C., Jr., & Bridge, H. S. 1981, J. Geophys. Res., 86, 8157
Stix, T. H. 1992, Waves in Plasmas (2d ed.; Woodbury: AIP)
Straus, J. M., & Schulz, M. 1976, J. Geophys. Res., 81, 5822
Vasyliūnas, V. M., & Eviatar, A. 2000, Geophys. Res. Lett., 27, 2347
Volland, H. 1984, Atmospheric Electrodynamics (Heidelberg: Springer)
Volwerk, M., Kivelson, M. G., Khurana, K. K., & McPherron, R. L. 1999, J. Geophys. Res., 104, 14, 729
Wells, W. C., Borst, W. L., & Zipf, E. C. 1971, Chem. Phys. Lett., 12, 288
Williams, D. J., & Mauk, B. H. 1997, J. Geophys. Res., 102, 24, 283
Williams, D. J., Mauk, B. M., & McEntire, R. W. 1997a, Geophys. Res. Lett., 24, 2953
Williams, D. J., et al. 1997b, Geophys. Res. Lett., 24, 2163